Relating Interface Properties with Crack Propagation in Composite Laminates

Tao Qu, Chandra Prakash, Vikas Tomar

Abstract—The interfaces between organic and inorganic phases in natural materials have been shown to be a key factor contributing to their high performance. This work analyzes crack propagation in a 2-ply laminate subjected to uniaxial tensile mode-I crack propagation loading that has laminate properties derived based on biological material constituents (marine exoskeleton- chitin and calcite). Interfaces in such laminates are explicitly modeled based on earlier molecular simulations performed by authors. Extended finite element method and cohesive zone modeling based simulations coupled with theoretical analysis are used to analyze crack propagation. Analyses explicitly quantify the effect that interface mechanical property variation has on the delamination as well as the transverse crack propagation in examined 2-ply laminates.

Keywords—Chitin, composites, interfaces, fracture.

I. INTRODUCTION

RECENT developments in finite element models capable of predicting both transverse cracks and inter-laminar failure in composites have used the extended Finite Element Method (XFEM) for matrix micro cracks and the cohesive zone model (CZM) for delamination [1]-[5]. Efforts [6]-[9] have been taken to improve the inter-laminar fracture toughness of composite materials by design of the ply interface. However, the quantitative interface-mechanical relation to guide the interface optimization is not available [10]. Current work is a contribution in this area. Progressive damage analysis of the two-adjacent-ply structure from the biomimetic "helicoidal structure" [11], [12] and engineered quasi-isotropic laminates with various mismatch angles of fiber orientations [13] is performed through the meso-scale finite element modeling of laminate structure, where the individual piles are modeled as a number of discrete, homogeneous, anisotropic layers [5]. The methodology developed in this work is based on a combined XFEM and surface cohesive zone model (SCZM) approach through the non-linear finite element code, ABAQUS [14]. XFEM is used for transverse crack initiation and propagation and SCZM is used for delamination growth (inter-laminar failure) between plies.

II. METHOD

This study, through the three-dimensional (3D) meso-level finite element modeling of a series of tensile tests on 2-ply

Tao Qu and Chandra Prakash are with School of Aeronautics and Astronautics, Purdue University-IN, 47907, USA.

Vikas Tomar is with School of Aeronautics and Astronautics, Purdue University-IN, 47907, USA (phone: 765-494-3423; e-mail: tomar@purdue.edu).

laminates, [5], (Fig. 1 (c), ~μm), predicts the influence of interface (inter-laminar) properties and lamellae fiber orientation on the related fracture resistance. Each lamina is made up of the basic organic (i.e. chitin, the fiber material) and inorganic (i.e. calcite, the matrix material) constituents of the marine exoskeleton materials. The basic problem consists of two plies with a sandwiched interface having a through thickness crack. Three different types of interface properties are given as the input to the finite element framework according to the changes in the chemical configuration of the CHI-CAL bio-interfaces based on previous molecular mechanics' studies [15]-[17]. Fracture resistance analyses involve transverse cracks and delamination. The loading is perpendicular so as to simulate a mode-I crack. Analyses incorporate an XFEM based approach to predict crack propagation in laminates and cohesive zone modeling based approach to predict crack propagation through interface between lamellae. During loading, both the lamellae and interface failure criterion are active. Crack propagation either occurs in lamellae or in interface based on the satisfaction of respective laminate or interface crack propagation criterion.

III. RESULTS

Engineering stress-strain relation for each structure with three different types of interfaces is calculated from the load-displacement data obtained from the simulations. The stress-strain curve for the [30°/90°] structure, with the simulation snapshots of progressive transverse crack and delamination is shown in Fig. 1. The first cracking initiation occurs in the 90° ply, which is the matrix crack according to the simulation snapshot illustrated in Fig. 1 (a). Then, delamination area is formed with the growth of the transverse crack propagation. As the stress increases, the second cracking initiation occurs in the 30° ply, of which the mode is fiber failure according to the simulation snapshot seen in Fig. 1 (b). At the last stage, a significant drop in the load occurs with the debonding of the interface and the breakage of each ply (see Fig. 1 (c)) just after the point of maximum strength has reached.

For all the simulated structures, the curves exhibit drastic drops after the maximum loading point, and this is a characteristic of the propagation instability phenomenon reported generally in shear mode of fracture (mode II) [18]. The strength for each structure is measured as the maximum engineering stress from the stress-strain curve. Fig. 2 shows the strength as a function of the incline angle for different mismatch angle structures with the three types of interfaces. According to the current simulations, the failure mode of 0° and 30° plies is predicted as the fiber failure and the failure mode of 60° and 90° plies is predicted as the matrix crack. At

θ_{mis} =30°, as the incline angle increases, the corresponding structures are [0°/30°], where both of constituent plies fail under the fiber failure mode, [30°/60°], whereas one of the constituent plies fails under the fiber failure mode and the other fails under the matrix crack mode, and [60°/90°], where both of the constituent plies fail under the matrix crack mode. Therefore, as expected the peak strength decreases with increasing of the incline angle (see Fig. 2 (a)). Similarly, different combinations of failure modes of the constituent plies lead to the variations of the peak strength of the structures as the function of incline angle at θ_{mis} =60° and 90° as shown in Figs. 2 (b) and (c). However, based on the simulation results, there is no significant effect of interface on the strength properties of the simulated 2-ply structures.
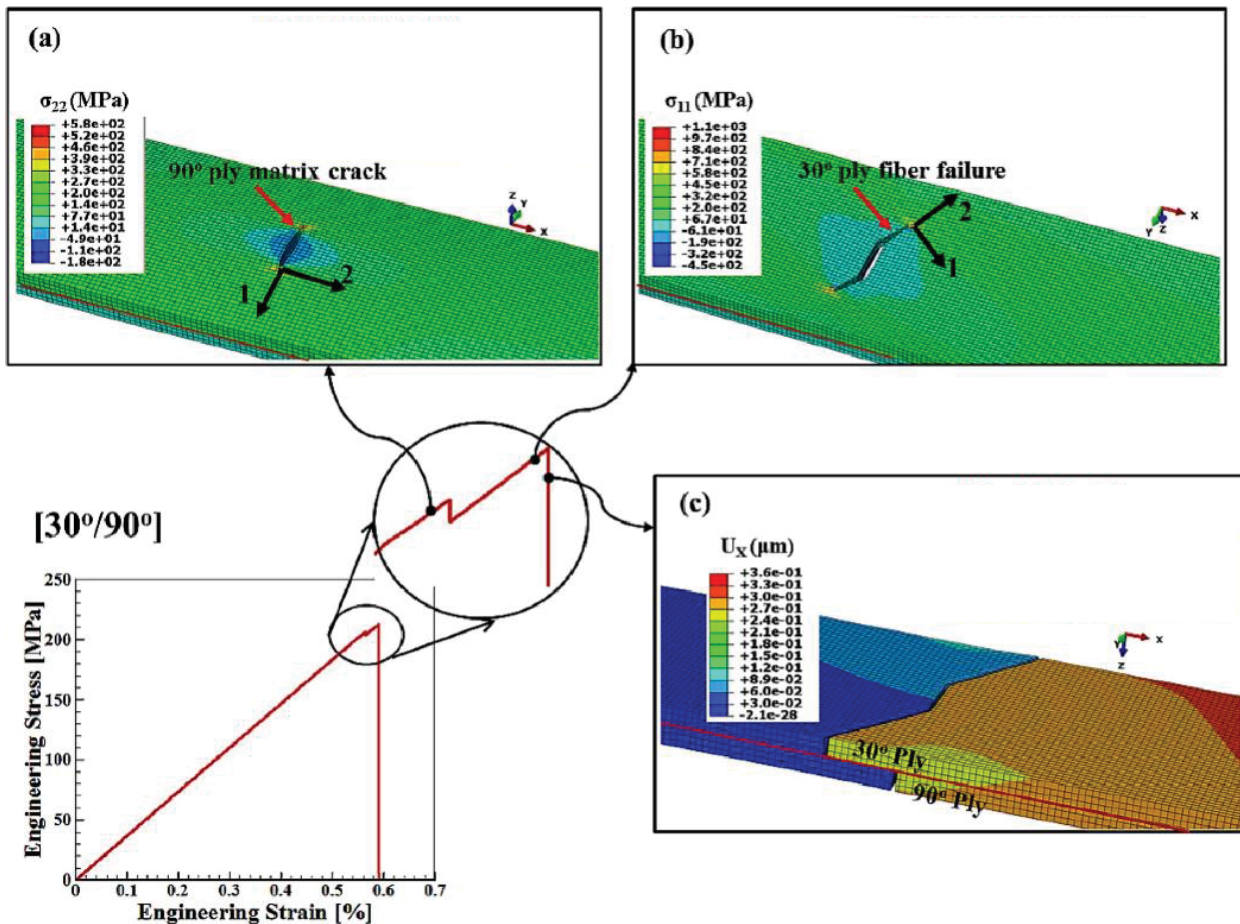

Fig. 1 Engineering stress-strain curve for the [30°/90°] example with simulation snapshots for the progressive damage in the laminated structure (a) matrix crack on the 90° ply, (b) fiber failure on the 30° ply, (c) the final status of the damage process
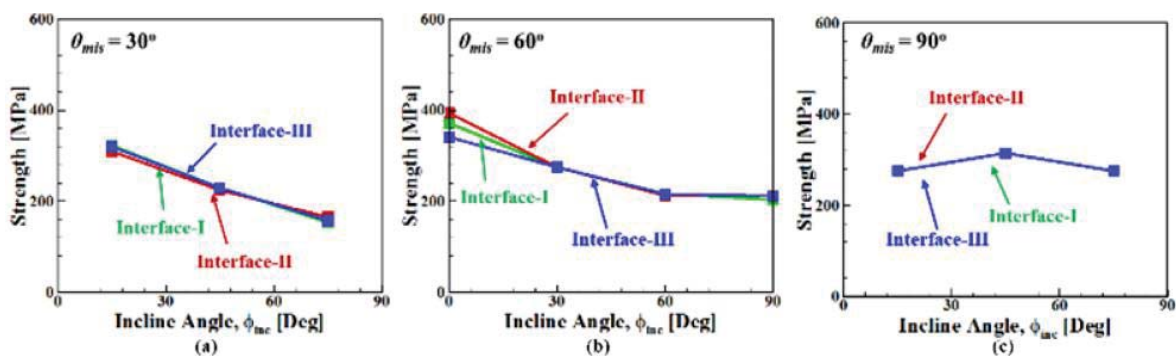

Fig. 2 Strength vs incline angle with different types of interface (a) mismatch angle =30°, (b) mismatch angle =60°, and (c) mismatch angle =90°

Generally, three cases of delamination shape are considered. Fig. 3 (a)-(c) show schematics of typical delamination shapes. When both of the plies exhibit the same failure mode, i.e. the crack paths are on the same side of the central line, the delamination shapes are smaller triangle shapes (see Fig. 3 (a), such as [0°/60°], [30°/90°], etc.). When the two plies exhibit different failure modes (one is fiber failure and one is matrix crack) or in the cases of angle-ply (i.e. [60°/-60°]), i.e. the crack paths are on different sides of the central line, the delamination shapes are larger triangle shapes (see Fig. 6 (b), such as [30°/60°] etc.). When the cracks propagate along the same path on both of the plies, the delamination area is much smaller than the other two cases, such as [0°/90°] and [30°/-60°]. The triangle area is related to the delamination fracture toughness and could be used as an indicator of the trend of the fracture toughness. Assuming plies with fiber orientation larger than 45° fail under matrix crack, Fig. 3 (d) shows the variation of the delamination triangle area as a function of the incline angle analytically based on the above discussions when mismatch angle θ_{mis} =30°. The discontinuity and the variation affect the delamination fracture toughness, which is discussed as follows.

In fracture mechanics, the energy release rate (ERR) is defined as the energy dissipated during fracture per unit of newly created fracture surface area, (1),

$$G = -\frac{dU}{dA} \qquad (1)$$

In the current analysis, the strain energy was dissipated due to the intra-laminar crack propagation and the inter-laminar delamination process. Thus, we can define the ERR for interface, Γ_i, as the energy released to drive delamination, which is used to quantify the delamination resistance for structures. This ERR is calculated based on the energy balance consideration of the whole model in simulations, (2),

$$\Gamma_i = \frac{\text{ALLDMD} - \Gamma_P \cdot A_P}{A_D} \qquad (2)$$

where, $ALLDMD$ is the total dissipated energy obtained from simulations, Γ_P is the critical ERR for transverse crack, $\Gamma_P = G_{I,II,III} = 0.54$ J/m². A_D is the delamination area. A_P is the transverse crack surface area, which can be estimated by $A_P = h(s_1 + s_2)$, where h is the ply thickness, s_1 and s_2 are the lengths of the crack path for the two plies determined from simulations. Fig. 4 shows the plot of Γ_i as a function of incline angle for different mismatch angle structures with the three types of interfaces. The dependence of the incline angle (ϕ_{inc}) of the ERR (Γ_i) is much more complicated than that of the strength. One could be predicted as follows. Since the ERR for transverse crack is much lower comparing with delamination ERR in the current studies, the delamination ERR could be approximated as the ratio of the total strain energy of the structure to the delamination area.
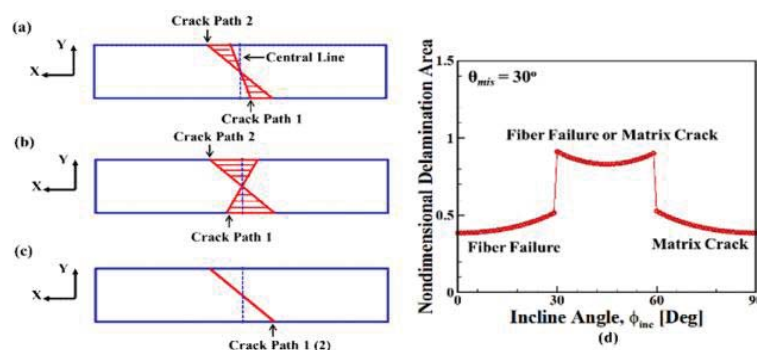

Fig. 3 A schematic (a), (b) and (c) showing three typical cases of delamination shape, (d) analytical prediction for the delamination area as a function of incline angle for the structures with the mismatch angle =30°
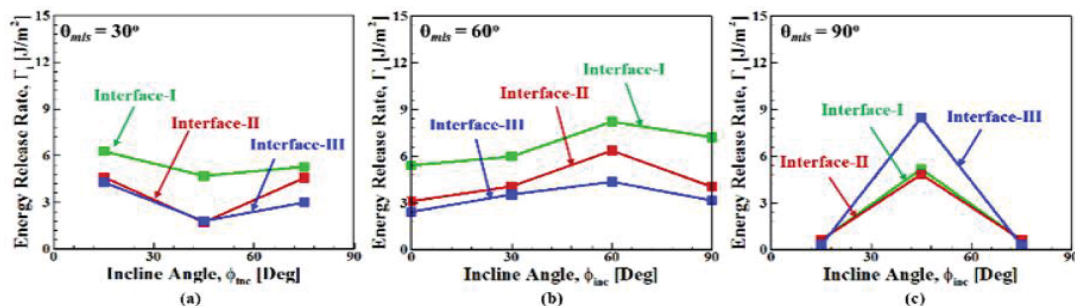

Fig. 4 Energy release rate for delamination (Γ_i) as a function of incline angle (ϕ_{inc}) with different types of interfaces for (a) mismatch angle =30°, (b) mismatch angle =60°, and (c) mismatch angle =90°

The structure exhibits linear elastic behavior till failure as observed from the stress-strain curve shown in Fig. 4. The total strain energy can be estimated as

$$U = eV , \qquad (3)$$

where V is the volume of the structure and e is the strain energy density which can be approximated as

$$e = \frac{1}{2} \frac{\sigma_X h}{A_{11}} \sigma_X , \qquad (4)$$

where h is the ply thickness, σ_X is the maximum strength. A_{11} is the extensional stiffness of the laminate structure,

$$A_{11} = (\bar{Q}_{11}^{(1)} + \bar{Q}_{11}^{(2)})h , \qquad (5)$$

where $\bar{Q}_{11}^{(1)}$ and $\bar{Q}_{11}^{(2)}$ are the elastic constants of first and second ply in the global coordinate system, respectively, which is angle (θ_{mis} and ϕ_{inc}) dependent.
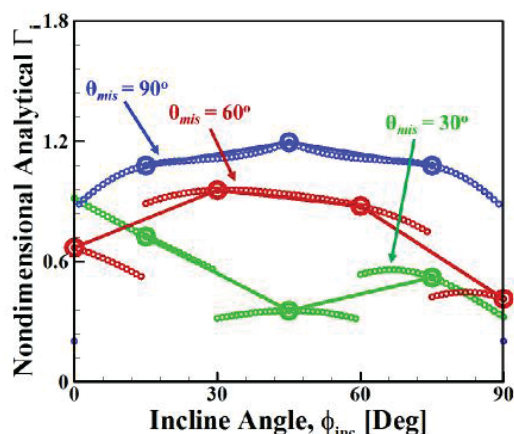

Fig. 5 Analytical approximation of the energy release rate for delamination (Γ_i) as a function of incline angle (ϕ_{inc}) for the structures with mismatch angle =30°, 60° and 90°

Finally, the delamination area could be analytically approximated based on the analysis shown earlier in Fig. 3. Fig. 5 shows the analytical approximations of ERR for delamination for the structures with different θ_{mis}. The trend agrees with the results obtained from simulations as shown in Fig. 5 (a)-(c). In order to further look into the influence of the interface, Γ_i will be derived analytically from the perspective of mode mix and CZM. In current study, we adopt the bilinear traction-separation law for the interfacial fracture.

REFERENCES

[1] Van der Meer, F., Sluys, L., Hallett, S., and Wisnom, M., "Computational modeling of complex failure mechanisms in laminates". *Journal of Composite Materials*, 2011: p. 0021998311410473.
[2] Iarve, E.V., Gurvich, M.R., Mollenhauer, D.H., Rose, C.A., and Dávila, C.G., "Mesh-independent matrix cracking and delamination modeling in laminated composites". *International journal for numerical methods in engineering*, 2011. 88(8): p. 749-773.
[3] Hallett, S.R., Jiang, W.-G., Khan, B., and Wisnom, M.R., "Modelling the interaction between matrix cracks and delamination damage in scaled quasi-isotropic specimens". *Composites Science and Technology*, 2008. 68(1): p. 80-89.
[4] Grogan, D., Brádaigh, C.Ó., and Leen, S., "A combined XFEM and cohesive zone model for composite laminate microcracking and permeability". *Composite Structures*, 2015. 120: p. 246-261.
[5] Rose, C.A., Davila, C.G., and Leone, F.A., "Analysis Methods for Progressive Damage of Composite Structures". 2013.
[6] Woolstencroft, D.H., "Composite". 2005, Google Patents.
[7] McMillan, A.J., "Component comprising a resin matrix". 2014, Google Patents.
[8] Chen, Z. and Mecholsky, J., "Control of strength and toughness of ceramic/metal laminates using interface design". *Journal of Materials Research*, 1993. 8(9): p. 2362-2369.
[9] Nobumasa, H. and Shimizu, K., "Light-weight composite material". 1988, Google Patents.
[10] Kim, J.-K. and Mai, Y.-W., "Engineered interfaces in fiber reinforced composites". 1998: Elsevier.
[11] Raabe, D., Al-Sawalmih, A., Romano, P., Sachs, C., Brokmeier, H., Yi, S., Servos, G., and Hartwig, H. "Structure and crystallographic texture of arthropod bio-composites". in *Materials Science Forum*. 2005: Transtec Publications; 1999.
[12] Cheng, L., Wang, L., and Karlsson, A.M., "Image analyses of two crustacean exoskeletons and implications of the exoskeletal microstructure on the mechanical behavior". *Journal of Materials Research*, 2008. 23(11): p. 2854-2872.
[13] Kim, B.W. and Mayer, A.H., "Influence of fiber direction and mixed-mode ratio on delamination fracture toughness of carbon/epoxy laminates". *Composites Science and Technology*, 2003. 63(5): p. 695-713.
[14] Manual, A.U., "Version 6.13-2". *Dassault Systémes Simulia Corp., Providence, Rhode Island, USA*, 2013.
[15] Qu, T. and Tomar, V. "Nanomechanics based investigation into interface-thermomechanics of collagen and chitin based biomaterials". in *Society of Engineering Science 51st Annual Technical Meeting*. 2014. West Lafayette, IN.
[16] Qu, T., Verma, D., Shahidi, M., Pichler, B., Hellmich, C., and Tomar, V., "Mechanics of organic-inorganic biointerfaces—Implications for strength and creep properties". *MRS bulletin*, 2015. 40(04): p. 349-358.
[17] Qu, T., Verma, D., Alucozai, M., and Tomar, V., "Influence of Interfacial Interactions on Deformation Mechanism and Interface Viscosity in α-Chitin-Calcite Interfaces". *Acta Biomaterialia*, 2015.
[18] Benzeggagh, M. and Kenane, M., "Measurement of mixed-mode delamination fracture toughness of unidirectional glass/epoxy composites with mixed-mode bending apparatus". *Composites Science and Technology*, 1996. 56(4): p. 439-449.